optica

Frequency-induced phase-tunable polarization-entangled narrowband biphotons

PENG CHEN, XIANXIN GUO, CHI SHU, M. M. T. LOY, AND SHENGWANG DU*

Department of Physics, The Hong Kong University of Science and Technology, Clear Water Bay, Kowloon, Hong Kong, China
**Corresponding author: dusw@ust.hk*

Received 16 March 2015; revised 28 April 2015; accepted 28 April 2015 (Doc. ID 236255); published 18 May 2015

Manipulating polarization entanglement of paired photons is always of great interest for understanding the quantum nature of photons and exploring their applications in quantum information processing and quantum communication. Narrowband biphotons with polarization entanglement are especially important for a quantum network based on efficient photon–atom interactions. In most demonstrated cases, the polarization-entangled states are manipulated through the birefringent effect. In this Letter, we produce narrowband polarization-entangled biphotons from spontaneous four-wave mixing in cold atoms and demonstrate a new method to tune the phase of the polarization entanglement by varying the frequency of one of the classical driving lasers. This is achieved through two-photon interference with a path-exchange symmetry. Our result represents a precision control of polarization entanglement from the frequency domain, and may have promising applications in quantum information and precision measurement.

OCIS codes: (270.0270) Quantum optics; (270.5585) Quantum information and processing; (190.4380) Nonlinear optics, four-wave mixing.

http://dx.doi.org/10.1364/OPTICA.2.000505

Entanglement, one of most delicate natures of quantum systems, plays a central role in quantum communication and quantum computation [1,2]. Photons, known as flying qubits, are ideal carriers for quantum entanglement because of their weak interaction with the environment. Photonic entanglement has been widely investigated in various degrees of freedom, such as polarization [3–5], energy (frequency)-time [6–8], momentum (path) [9], and orbital angular momentum [10,11]. Due to good accessibility and controllability, photonic polarization is the key resource for entanglement and prevalently utilized in nearly all aspects of quantum information and fundamentals of quantum mechanisms. Creation, manipulation, and characterization of polarization-entangled states is essential for these studies.

Usually, the relative phase (one of the intrinsic degrees of freedom) between the two components of polarization-entangled biphotons is controlled by the birefringence effect [2]. For example, four polarization-entangled Bell states can be mutually transferred through rotation of waveplates placed at the output of source in principle. For the polarization-entangled state generated from spontaneous parametric down-conversion, the relative phase can also be adjusted by tilting the down-conversion crystal itself [5]. Using two identical nonlinear crystals placed with the optical axes orthogonal to each other, Kwiat *et al.* showed that the relative phase can be directly tuned with the polarization of the pump laser [12]. The same method was also employed to transfer different polarization-entangled Bell states from spontaneous four-wave mixing (SFWM) in a fiber loop [13]. However, the broadband spectra of these sources, typically on the order of THz, make it hard to tune the relative phase with frequency. As the birefringence effect is strongly dependent on the temperature [14], dynamic control of the relative phase with precision and long-term stability still remains a challenge.

In recent years, SFWM with electromagnetically induced transparency in cold atoms has become an efficient method to produce narrowband biphotons [15–17]. Narrowband biphotons with coherence time exceeding 1 μs have been reported [18,19]. By employing spatial symmetry either from the production or collection process in the SFWM, polarization-entangled narrowband biphotons have been achieved [20–23]. In particular, Shu *et al.* show a convenient way to transfer the polarization-induced phase into frequency-bin entanglement without the need of path locking [23].

In this Letter, we demonstrate the generation of polarization-entangled narrowband biphotons from SFWM in cold atoms with tunable phase by varying the frequency of the pump laser. Using a scheme of two-photon interference with path-exchange symmetry, we obtain polarization entanglement for narrowband biphotons. We show that the relative phase varies linearly with the detuning of the pump laser. For the first time to our knowledge, we show the controllability of the inner freedom of polarization entanglement from the frequency domain. So far as we know, all previous two-photon interference experiments have been implemented through path difference adjustment or polarization rotation; our method is a new way to control the two-photon interference by adjusting the photon frequency [24,25].

The experimental setup and atomic energy level diagram are shown in Figs. 1(a) and 1(b). Narrowband paired Stokes (ω_s) and anti-Stokes (ω_{as}) photons are generated from SFWM in cold ^{85}Rb atoms loaded in a three-dimensional magneto-optical trap [26,27]. The pump laser (ω_p, 60 mW, diameter 2 mm) is far blue

detuned from the atomic transition $|1\rangle \rightarrow |3\rangle$ by an adjustable Δ_p. The coupling laser (ω_c, 3 mW, diameter 2 mm) is resonant on the transition $|2\rangle \rightarrow |3\rangle$. The Stokes and anti-Stokes photons are associated with the transitions $|3\rangle \rightarrow |2\rangle$ and $|3\rangle \rightarrow |1\rangle$, respectively. The atoms are initially prepared in the ground state $|1\rangle$ with an optical depth of about 3 on the transition $|3\rangle \rightarrow |1\rangle$. $\Delta_{21} = 2\pi \times 3036$ MHz is the hyperfine splitting of two ground states. The linearly polarized pump and coupling lasers are counterpropagating to establish a backward configuration of SFWM. The phase-matched backward-paired photons are collected at a right angle with respect to the propagation direction of pump and coupling lasers. Such a right-angle geometry of collection allows path-exchange symmetry for emitted photon pairs: the Stokes photons can go to the left (path 1) and the anti-Stokes photons go to the right (path 2), and vice versa. The generated photon pairs are then coupled by a beam splitter (BS) with different orthogonal polarizations. The polarizations of photons are selected to be horizontal (H) in path 1 and vertical (V) in path 2, respectively. After passing through two polarizers P_3 and P_4, the output paired photons from the BS are coupled into two single-mode fibers (SMFs), and finally detected by two single-photon counting modules (Excelitas SPCM-AQRH-16-FC). Both P_3 and P_4 are composed of a $\lambda/4$-wave, $\lambda/2$-wave, and polarizing beam splitter.

The polarization state of paired photons output from ports 3 and 4 of the BS is entangled under the condition of coincidence measurement shown in Fig. 1(a). As path 1 and path 2 are associated with different polarizations, photons can have two random choices of polarization in H or V with equal probability after BS. Since only the paired photons at different ports are measured in coincidence measurement, the polarization state of paired photons must be the Bell-type entangled state $(|\mathrm{HV}\rangle + e^{i\phi}|\mathrm{VH}\rangle)/\sqrt{2}$, where ϕ is the relative phase between the two components of the state. Taking into account the temporal wave packet of paired photons in the time domain, the two-photon state in the Schrödinger picture is [26,27]

$$\begin{aligned}|\Psi(t_s, t_{as})\rangle = \frac{e^{iA}}{\sqrt{2}}[&\varphi(\tau - \Delta t)e^{-i\Delta\omega(\tau-\Delta t)/2}|\mathrm{HV}\rangle \\ &+ \varphi(\tau + \Delta t)e^{-i\Delta\omega(\tau+\Delta t)/2}|\mathrm{VH}\rangle \\ &+ \varphi(-\tau - \Delta t)e^{i\Delta\omega(\tau+\Delta t)/2}|\mathrm{VH}\rangle \\ &+ \varphi(-\tau + \Delta t)e^{i\Delta\omega(\tau-\Delta t)/2}|\mathrm{HV}\rangle], \end{aligned} \quad (1)$$

where $\tau = t_{as} - t_s$. e^{iA} is a fast global phase that has no effect on the experiment. $\varphi(\tau)$, nonzero only for $\tau > 0$ caused by the time ordering of the SFWM process, is the single-side two-photon relative wave function without path-exchange symmetry [17]. The Stokes photon always comes out before its paired anti-Stokes photon. $\Delta t = t_2 - t_1$ is the relative time delay between path 1 and path 2, and $\Delta\omega = \Delta_{21} - \Delta_p$ is the central frequency difference between the anti-Stokes and Stokes photons. In our experiment, we set Δt much shorter than the two-photon coherent time of $\varphi(\tau)$ such that $\varphi(\tau - \Delta t) \approx \varphi(\tau + \Delta t) \approx \varphi(\tau)$. Thus, the positive part of $\tau > 0$ in Eq. (1) can be further simplified as

$$|\Psi(\tau > 0)\rangle = \frac{e^{iA}}{\sqrt{2}}\varphi(\tau)e^{-i\Delta\omega(\tau-\Delta t)/2} \times [|\mathrm{HV}\rangle + e^{-i\Delta\omega\Delta t}|\mathrm{VH}\rangle], \quad (2)$$

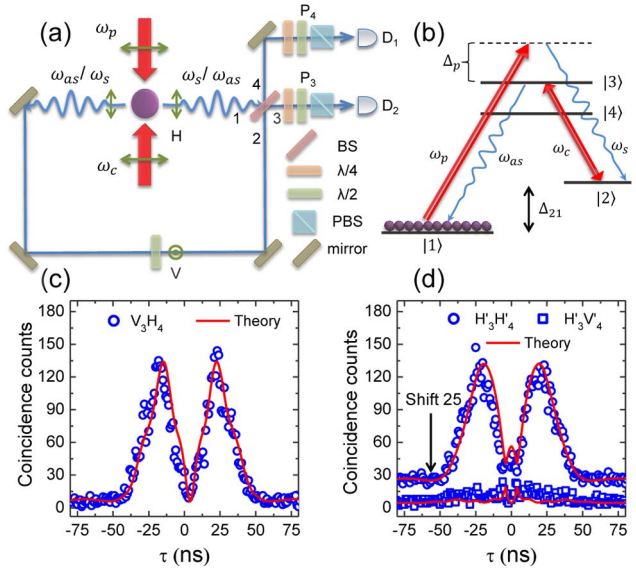

Fig. 1. (a) Schematic of experimental setup for generation of narrowband polarization-entangled paired photons from SFWM in cold atoms. The phase-matched paired photons are collected with a right-angle geometry in the backward configuration of SFWM. (b) ^{85}Rb D_2 line energy level diagram in the SFWM. The relevant energy levels are $|1\rangle = |5S_{1/2}, F = 2\rangle$, $|2\rangle = |5S_{1/2}, F = 3\rangle$, $|3\rangle = |5P_{3/2}, F = 3\rangle$, and $|4\rangle = |5P_{3/2}, F = 2\rangle$, respectively. Both the pump and coupling lasers work at 780 nm. (c) Two-photon coincidence counts measured with $P_3 = \mathrm{V}$, $P_4 = \mathrm{H}$ as a function of the relative time delay τ. (d) Two-photon coincidence counts measured with $P_3 = \mathrm{H}'$, $P_4 = \mathrm{H}'$ (blue circles) and $P_3 = \mathrm{H}'$, $P_4 = \mathrm{V}'$ (blue squares) as functions of the relative time delay τ. The blue circles are shifted upward by 25 counts to distinguish with the blue squares. In both (c) and (d), theoretical curves are calculated using Eq. (1) with a common scale factor.

which is a Bell-type polarization-entangled state whose temporal amplitude is determined by the single-side wave function $\phi(\tau)$. The relative phase ϕ is given by $-\Delta\omega\Delta t$. Because the central frequency of the Stokes photon is determined by the detuning of the pump laser, it could be expected that the relative phase ϕ can be varied by tuning the frequency of pump laser. As for the negative part of $\tau < 0$ in Eq. (1), the relative phase is found to $\Delta\omega\Delta t$, the sign of which is opposite to the case of $\tau > 0$. For convenience, we will only discuss the positive part in the following. In the experiment, the positive or negative part can be distinguished by time-ordering information or narrowband filters which only choose the Stokes or anti-Stokes photons in the coincidence measurement. Figures 1(c) and 1(d) show that two-photon coincidence patterns are measured with different polarization bases of P_3 and P_4. The polarization projection is chosen to be $|\mathrm{V_3H_4}\rangle\langle\mathrm{H_4V_3}|$ in Fig. 1(c) and $|\mathrm{H_3'H_4'}\rangle\langle\mathrm{H_4'H_3'}|$, $|\mathrm{H_3'V_4'}\rangle\langle\mathrm{V_4'H_3'}|$ in Fig. 1(d), where $|\mathrm{H}'\rangle = (|\mathrm{H}\rangle + |\mathrm{V}\rangle)/\sqrt{2}$ and $|\mathrm{V}'\rangle = (|\mathrm{H}\rangle - |\mathrm{V}\rangle)/\sqrt{2}$. The $\Delta\omega$ is set to $\approx$0 MHz by tuning the pump $\Delta_p = \Delta_{21} - 2\pi \times 1$ MHz, where the additional pump detuning is used to compensate the frequency shift of the ground state from the AC Stark effect and the magnetic-field-induced Zeeman effect [27]. The relative time delay Δt is kept to -4.2 ns by inserting an approximately 1 m long SMF in path 1. In Fig. 1(c), the coincidence counts show no interference pattern with a slightly shifted temporal zero

point, as only one polarization base is selected [see the second and third terms in Eq. (1)]. However, coincidence counts in Fig. 1(d) show high or almost no two-photon signals due to the polarization entanglement and agree well with theoretical prediction.

Next, we show two particular cases where the relative phase in polarization entanglement is controlled by pump laser detuning. First, we set $\Delta\omega \approx 0$ MHz with the same condition in Figs. 1(c) and 1(d). In this case, the relative phase ϕ turns to zero. Thus the polarization-entangled state of paired photons is $\Psi^+ = (|\mathrm{HV}\rangle + |\mathrm{VH}\rangle)/\sqrt{2}$. To get full information of density matrix of the polarization state, we measure 16 independent coincidence counts with the polarization quantum-state tomography [28]. The coincidence counts of each set are integrated in the range from ± 8 to ± 32 ns within the two-photon coherence time. The density matrix reconstructed using the maximum likelihood estimation method is

$$\begin{pmatrix} 0.053 & -0.029+0.048i & -0.062+0.011i & 0.015-0.007i \\ -0.029-0.048i & 0.434 & 0.375+0.057i & 0.051-0.02i \\ -0.063-0.011i & 0.375-0.057i & 0.466 & 0.009-0.051 \\ 0.015+0.007i & 0.051+0.02i & 0.009+0.051i & 0.047 \end{pmatrix},$$

of which graphical representation is shown in Fig. 2(a). The fidelity between the experimental result and the ideal state Ψ^+ is 82.5%. Further with the reconstructed density matrix, we test the violation of the Bell–CHSH inequality ($|S| \leq 2$) and obtain $S = 2.23 \pm 0.04$ [29]. Second, we tune Δ_p to $\Delta_{21} + 2\pi \times 119$ MHz so that $-\Delta\omega\Delta t \approx -\pi$. Thus, we obtain another Bell-type state $\Psi^- = (|\mathrm{HV}\rangle - |\mathrm{VH}\rangle)/\sqrt{2}$. The reconstructed density matrix with the maximum likelihood estimation method is

$$\begin{pmatrix} 0.025 & 0.014-0.047i & -0.012+0.043i & 0.012-0.004i \\ 0.014+0.047i & 0.457 & -0.414+0.071i & 0.037+0.011i \\ -0.012-0.043i & -0.414-0.071i & 0.497 & -0.008-0.025i \\ 0.012+0.004i & 0.037-0.011i & -0.008+0.025i & 0.021 \end{pmatrix}.$$

Figure 2(b) shows the corresponding graphical representation. We get a fidelity of 89.1% with the ideal state Ψ^- and obtain $S = 2.42 \pm 0.05$ for violation of Bell–CHSH inequality. Both cases show that a high fidelity with the desired state with different relative phase can be achieved by changing the pump laser frequency.

To further confirm that the relative phase can be freely manipulated by tuning the frequency of the pump laser, we scan the pump detuning in the range from -3 MHz $+ \Delta_{21}$ to 247 MHz $+ \Delta_{21}$ ($\Delta t = -4.2$ ns) with a fixed frequency step $\Delta\omega_{\mathrm{step}} = 25$ MHz. By measuring the two-photon coincidence counts ($\tau > 0$) with two set of polarizer $P_3 = H'$, $P_4 = H'$ and $P_3 = H'$, $P_4 = V'$, we can get $\cos\phi = \frac{1}{\eta}\frac{C-D}{C+D}$, where η ($0 < \eta \leq 1$) is the co-efficient of visibility and C and D are the integrated coincidence counts with $P_3 = H'$, $P_4 = H'$ and $P_3 = H'$, $P_4 = V'$, respectively. Figure 3(a) shows $\cos\phi$ is as a function of the detuning of pump laser. The theoretical curve is drawn with $\eta\cos(\Delta\omega\Delta t)$ in Fig. 3(a). Taking into account $\Delta\omega_{\mathrm{step}}\Delta t = -0.21\pi < 0$, we can fully determine the relative phase ϕ, as shown in Fig. 3(b), where the relative phase ϕ shifts linearly with the detuning of pump laser. The experimental result agrees well with the theory. We estimate the generation rate of polarization-entangled photon pairs for the condition of Fig. 3 is about 360 pairs/s, according to the channel transmission (27%), fiber coupling efficiency (70%), quantum efficiency of detector (50%), and duty cycle (33%). Because the paired photon rate scales with $1/\Delta_p^2$, it is quite insensitive to the far detuning of the pump laser.

During the experiment, we notice that the relative phase is very sensitive to the detuning of the pump laser. In our case, even a variation of 5 MHz in pump detuning can cause a phase shift of 7.56°. For a longer relative time delay between paths 1 and 2 within the two-photon coherence time, the phase variation can be more significant. Thus, our method can applied to precisely measure the frequency degeneracy of two paired single photons. As seen in Eqs. (1) and (2), there is polarization-dependent two-photon interference associated with polarization entanglement, induced by the path-exchange symmetry. We also demonstrate controlling two-photon interference by directly varying their frequencies without using the birefringence effect or path difference adjustment.

In summary, we demonstrate the generation of narrowband biphotons with polarization entanglement whose relative phase can be controlled by tuning the pump laser frequency. The relative phase is determined by the product of frequency difference of paired photons and the relative time delay between the two paths, and thus changes linearly with the pump laser frequency.

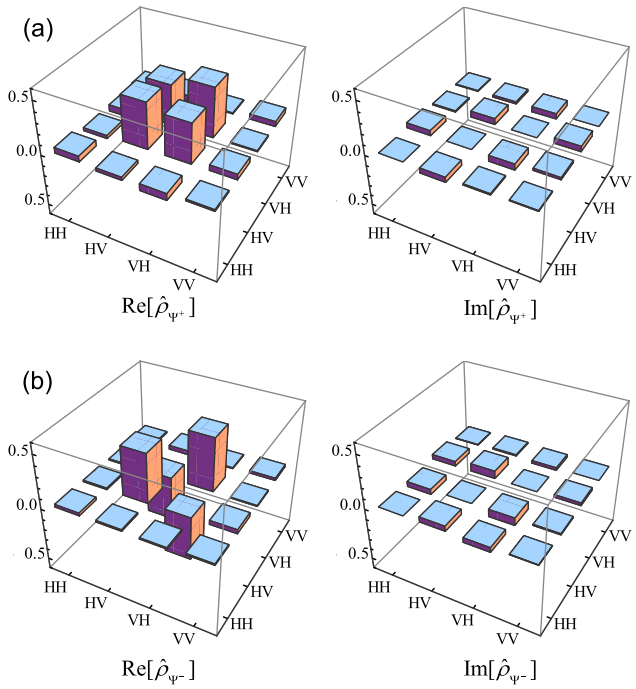

Fig. 2. Tomography measurement results at the target states of (a) Ψ^+ and (b) Ψ^-. Only the pump laser detuning is changed in the two cases. As both positive and negative parts have the same relative phase, we use the double-side coincidence counts in the tomography measurement.

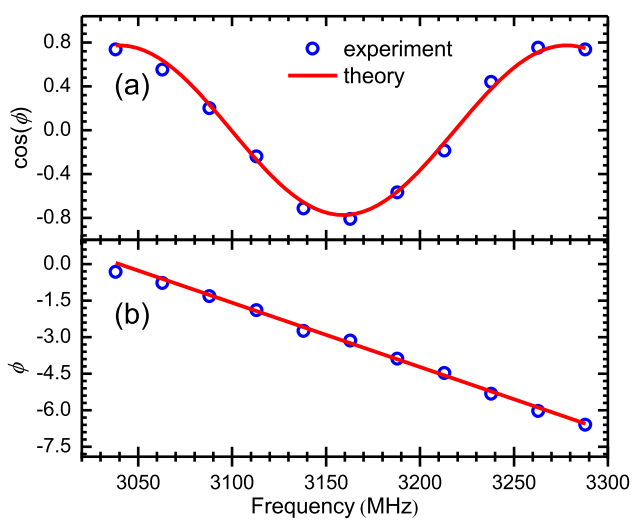

Fig. 3. Relative phase ϕ as a function of the pump laser detuning. The start point is at 3038 MHz and the frequency step is fixed to be 25 MHz. (a) cos ϕ, (b) ϕ.

As the laser frequency can be stabilized and measured with an accuracy down to mHz [30], our technique can be applied to precisely control polarization entanglement and manipulate two-photon interference.

Hong Kong Research Grants Council (601113).

REFERENCES

1. R. Horodecki, P. Horodecki, M. Horodecki, and K. Horodecki, Rev. Mod. Phys. **81**, 865 (2009).
2. J.-W. Pan, Z.-B. Chen, C.-Y. Lu, H. Weinfurter, A. Zeilinger, and M. Żukowski, Rev. Mod. Phys. **84**, 777 (2012).
3. Z. Y. Ou and L. Mandel, Phys. Rev. Lett. **61**, 50 (1988).
4. Y. H. Shih and C. O. Alley, Phys. Rev. Lett. **61**, 2921 (1988).
5. P. G. Kwiat, K. Mattle, H. Weinfurter, A. Zeilinger, A. V. Sergienko, and Y. Shih, Phys. Rev. Lett. **75**, 4337 (1995).
6. J. D. Franson, Phys. Rev. Lett. **62**, 2205 (1989).
7. J. Brendel, N. Gisin, W. Tittel, and H. Zbinden, Phys. Rev. Lett. **82**, 2594 (1999).
8. S. Ramelow, L. Ratschbacher, A. Fedrizzi, N. K. Langford, and A. Zeilinger, Phys. Rev. Lett. **103**, 253601 (2009).
9. J. G. Rarity and P. R. Tapster, Phys. Rev. Lett. **64**, 2495 (1990).
10. A. Mair, A. Vaziri, G. Weihs, and A. Zeilinger, Nature **412**, 313 (2001).
11. M. Lassen, G. Leuchs, and U. L. Andersen, Phys. Rev. Lett. **102**, 163602 (2009).
12. P. G. Kwiat, E. Waks, A. G. White, I. Appelbaum, and P. H. Eberhard, Phys. Rev. A **60**, R773 (1999).
13. H. Takesue and K. Inoue, Phys. Rev. A **70**, 031802R (2004).
14. J. Snoddy, Y. Li, F. Ravet, and X. Bao, Appl. Opt. **46**, 1482 (2007).
15. V. Balic, D. A. Braje, P. Kolchin, G. Y. Yin, and S. E. Harris, Phys. Rev. Lett. **94**, 183601 (2005).
16. S. Du, P. Kolchin, C. Belthangady, G. Y. Yin, and S. E. Harris, Phys. Rev. Lett. **100**, 183603 (2008).
17. S. Du, J. Wen, and M. H. Rubin, J. Opt. Soc. Am. B **25**, C98 (2008).
18. L. Zhao, X. Guo, C. Liu, Y. Sun, M. M. T. Loy, and S. Du, Optica **1**, 84 (2014).
19. Z. Han, P. Qian, L. Zhou, J. F. Chen, and W. Zhang, Sci. Rep. **5**, 9126 (2015).
20. H. Yan, S. Zhang, J. F. Chen, M. M. T. Loy, G. K. L. Wong, and S. Du, Phys. Rev. Lett. **106**, 033601 (2011).
21. K. Liao, H. Yan, J. He, S. Du, Z.-M. Zhang, and S.-L. Zhu, Phys. Rev. Lett. **112**, 243602 (2014).
22. D. N. Matsukevich, T. Chanelie're, M. Bhattacharya, S.-Y. Lan, S. D. Jenkins, T. A. B. Kennedy, and A. Kuzmich, Phys. Rev. Lett. **95**, 040405 (2005).
23. C. Shu, X. Guo, P. Chen, M. M. T. Loy, and S. Du, Phys. Rev. A **91**, 043820 (2015).
24. C. K. Hong, Z. Y. Ou, and L. Mandel, Phys. Rev. Lett. **59**, 2044 (1987).
25. H. Jin, F. M. Liu, P. Xu, J. L. Xia, M. L. Zhong, Y. Yuan, J. W. Zhou, Y. X. Gong, W. Wang, and S. N. Zhu, Phys. Rev. Lett. **113**, 103601 (2014).
26. C. Liu, J. F. Chen, S. Zhang, S. Zhou, Y.-H. Kim, M. M. T. Loy, G. K. L. Wong, and S. Du, Phys. Rev. A **85**, 021803(R) (2012).
27. P. Chen, C. Shu, X. Guo, M. M. T. Loy, and S. Du, Phys. Rev. Lett. **114**, 010401 (2015).
28. D. F. V. James, P. G. Kwiat, W. J. Munro, and A. G. White, Phys. Rev. A **64**, 052312 (2001).
29. J. F. Clauser, M. A. Horne, A. Shimony, and R. A. Holt, Phys. Rev. Lett. **23**, 880 (1969).
30. T. Kessler, C. Hagemann, C. Grebing, T. Legero, U. Sterr, F. Riehle, M. J. Martin, L. Chen, and J. Ye, Nat. Photonics **6**, 687 (2012).